Water Air Soil Pollut (2024) 235:353
https://doi.org/10.1007/s11270-024-07159-5

Adsorption Characteristics And Mechanism of U(Vi) In Water By Dopamine Hydrochloride Modified Bentonite

Longxiang Li · Zhongkui Zhou · Yadan Guo · Yishuo Zhang · Yi Zhao · Yan Xin

Received: 1 February 2024 / Accepted: 9 May 2024 / Published online: 21 May 2024

Abstract In this study, bentonite (B) was modified by hydrochloric acid dopamine (PDA), and the modification was confirmed by XRD, SEM, EDS and thermogravimetric analysis. Hydrochloric acid dopamine modified bentonite (PDA-B) was synthesized by a facile one-step hydrothermal method, and the obtained material exhibited particle-like polydopamine protrusions on the surface, which were distinctly different from natural bentonite, suggesting that PDA-B had abundant adsorption sites on the surface, which could enhance its adsorption performance for low-concentration U (VI). Single-factor tests and orthogonal experiments were conducted to optimize the adsorption conditions. The ideal conditions for adsorbing uranium-containing wastewater with an initial concentration of 10 mg/L were found to be a pH of 7.0, PDA-B dosage (m) of 2 g/L, a reaction time (t) of 150 min, room temperature, and an agitation speed (R) of 150 r/min. Under these conditions, the removal rate exceeded 98%. Adsorption isotherms and kinetic models were applied to the data, revealing that the uranium adsorption process by PDA-B adhered to the Freundlich isotherm adsorption model and the pseudo-second-order kinetic model. The adsorption process was determined to be endothermic and spontaneous. The adsorption characteristics of U(VI) were extensively examined using FTIR, and Zeta potential analyses, shedding light on the underlying removal mechanism. The study found that hexavalent uranium was adsorbed, and multiple factors including carbonyl, amino, hydroxyl, electrostatic attraction, and ion exchange played pivotal roles in the adsorption of uranium by PDA-B. Additionally, reusability tests demonstrated its practical reusability. In summary, the PDA-B adsorbent exhibits promising application prospects and can be effectively utilized for the purification and recovery of uranium-containing wastewater.

Keywords Bentonite · Intropin · Uranium · Adsorption model · Adsorption mechanism

Supplementary Information The online version contains supplementary material available at https://doi.org/10.1007/s11270-024-07159-5.

L. Li · Z. Zhou (✉) · Y. Guo · Y. Zhang · Yi. Zhao · Y. Xin
State Key Laboratory of Nuclear Resources and Environment, East China University of Technology, 330013, Jiangxi, Nanchang, China
e-mail: zhkzhou80@163.com

L. Li · Z. Zhou · Y. Guo · Yi. Zhao · Y. Xin
Jiangxi Provincial Key Laboratory of Genesis and Remediation of Groundwater Pollution, East China University of Technology, 330013, Jiangxi, Nanchang, China

Y. Zhang
School of Nuclear Science and Engineering, East China University of Technology, 330013, Jiangxi, Nanchang, China

1 Introduction

Uranium, an essential element in the nuclear industry, plays an indispensable role in China's energy and

military sectors. The nuclear fuel cycle, uranium ore over-exploitation, improper treatment of spent fuel, and nuclear fuel manufacturing collectively generate a substantial amount of uranium-containing wastewater. This has resulted in uranium becoming a common metal pollutant in rivers, lakes, groundwater, and soil (Ma et al., 2022). Uranium is naturally radioactive and possesses an extraordinarily long half-life. Upon entering the human body, it undergoes decay and emits radiation, leading to internal radiation exposure and causing various severe health issues, including leukemia, kidney disease, lung disease, and even cancer. In its natural state, uranium exists in two valence states: hexavalent uranium [U(VI)] and tetravalent uranium [U(IV)] (Chen et al., 2023). Water commonly contains low concentrations of hexavalent uranium [U(VI)], which is more hazardous than its tetravalent counterpart [U(IV)]. This heightened toxicity, along with its increased solubility and mobility, accentuates the risks associated with U(VI) in water (Pentyala et al., 2020). If uranium persists in the ecosystem for extended periods without effective treatment and recycling, its distinctive radioactivity is bound to inflict irreversible harm on the entire ecosystem (Verma M. et al., 2024). Therefore, addressing the removal of low concentrations of U(VI) from water has become an urgent issue that requires resolution.

The removal of uranium from wastewater encompasses various methods, such as photocatalysis, oxidation–reduction processes, electrochemistry, chemical precipitation, flocculation, ion exchange, and adsorption. Among these, the adsorption method stands out due to its economic viability, ease of operation, high treatment efficiency, and environmental friendliness. Consequently, it has gained widespread use in treating uranium-containing wastewater. Presently, both domestically and internationally, materials used for adsorbing uranium from wastewater include resins, nano zero-valent iron, polymers, clay minerals (like attapulgite, diatomite, zeolite), metal hydroxides, and hydroxyapatite (Ma et al., 2022). While traditional adsorption techniques are capable of removing uranium from water, they suffer from drawbacks like inefficient recycling, intricate adsorbent preparation, and high costs. These limitations curtail their practical applicability in treating uranium-containing wastewater. The quest to develop low-cost adsorption materials characterized by stability, straightforward synthesis, and suitability for low-concentration uranium-containing wastewater has piqued the interest of the academic community. Consequently, the exploration of novel uranium adsorption materials holds great significance.

Bentonite is widely employed in the realm of environmental protection due to its array of advantages, including robust heat resistance, a generous specific surface area, high adsorption efficiency, substantial storage capacity, ease of regeneration, cost-effectiveness, environmental friendliness, and straightforward modification (Zhang et al., 2022a, 2022b). Nevertheless, the adsorption capacity of natural bentonite is constrained, necessitating optimization and modification to enhance its interlayer spacing and surface functional groups for improved adsorption performance. Currently, the modification of bentonite encompasses techniques such as acidification, roasting, salt activation, sodium modification, the addition of modifiers, and compounding (Mahadevan et al., 2020). For instance, the modification of bentonite with calcium chloride has been employed to eliminate organic pollutants from water (Lian et al., 2009). To efficiently remove the heavy metal pollutant Cr^{3+}, the pillaring method can be used to modify bentonite, resulting in a twofold increase in the adsorption capacity for Cr^{3+} compared to natural bentonite (Volzone et al., 2008). However, these studies primarily focus on enhancing the specific surface area and interlayer spacing of bentonite while neglecting the chelation and coordination potential of functional groups.

This work details the modification of bentonite through the introduction of dopamine hydrochloride, which contains a multitude of functional groups. The outcome of this process is the successful creation of dopamine hydrochloride-modified bentonite, referred to as PDA-B. This modification not only enhances the interlayer spacing of bentonite but also introduces functional groups with potent chelating capabilities for metals.

The adsorption process of PDA-B was thoroughly examined using inductively coupled plasma emission spectrometry (ICP-OES). Furthermore, the adsorption characteristics of PDA-B for uranium were investigated by applying various models, including isothermal adsorption models, thermodynamic models, and kinetic models. Characterization techniques were also employed to unveil the underlying adsorption mechanisms, thereby providing

substantial data and evidence to support the efficient removal of low concentrations of uranium from wastewater.

2 Materials and Methods

2.1 Preparation of PDA-B

The commercial activated carbon used in this study was obtained from Tianjin Beichen Fangzheng Reagent Factory. Sodium bentonite was prepared according to the method described in Reference (Zhang et al., 2022a, 2022b). The Al-pillared bentonite was synthesized as per the procedure outlined in Reference (Zhou et al., 2012). Similarly, the preparation of Fe and Ti pillared bentonite followed the methodology detailed in Reference (Xiong et al., 2018), and CTAB iron pillared bentonite was produced using the approach found in literature (Shu et al., 2021). To prepare PDA-B, the following steps were taken: An appropriate quantity of dopamine hydrochloride was dissolved in ultrapure water and stirred continuously under vacuum to ensure complete dissolution. The pH of the system was adjusted to weak alkalinity (approximately 8.5) by adding diluted NaOH. Natural bentonite, without sodium modification, was accurately weighed and gradually introduced into the dopamine hydrochloride solution. Continuous stirring was maintained to ensure thorough mixing with dopamine hydrochloride. The reaction system was vacuum-sealed and temperature-controlled at 353.15 K, with stirring continued for 480 min. The system was then allowed to cool to room temperature naturally, followed by filtration, centrifugation, and washing. The washing process continued until the supernatant reached a neutral pH and the system appeared nearly colorless. The resulting material was then placed in a vacuum drying oven at 353.15 K for drying. Subsequently, it was ground and passed through a 100 μm sieve to yield brown-black powder, which is referred to as dopamine hydrochloride-modified bentonite, denoted as PDA-B.

2.2 Analytical Methods

Bentonite, dopamine hydrochloride, uranium standard solution, 5% nitric acid (used for ICP-OES diluted samples), hydrochloric acid and sodium hydroxide were all analytically pure. The test used 10 mg/L uranium, which was diluted with uranium standard solution and ultrapure water.

The adsorption experiments were conducted using a batch method with water bath shaking. Different masses of PDA-B were weighed and added to 100 mL conical flasks. Then, 50 mL of U(VI)-contaminated wastewater with a certain concentration and pH value was added. The mixture was stirred at a predetermined temperature and speed for a specific duration. After shaking, samples were immediately taken and filtered through a 0.22 μm membrane filter and centrifuged. The remaining U(VI) concentration was determined using ICP-OES. Three parallel experiments were conducted, and the average value was taken as the result. The removal efficiency (η) of U(VI) was calculated using equations respectively:

$$\eta = (C_0 - C_e)/C_0 \times 100\%$$

where η represents the removal efficiency of U(VI) (%), C_0 and C_e are the initial and equilibrium mass concentrations of U(VI) (mg/L).

The natural bentonite, PDA-B, and uranium-adsorbed PDA-B were characterized using SE), XRD, FTIR, XPS, Zeta potential analyzer, and EDS. The characterization of PDA-B corresponded to the adsorption conditions of an initial U(VI) concentration of 10 mg/L, water sample pH of 7.0, agitation rate of 150 r/min, room temperature, and adsorption time of 300 min.

3 Results and Discussion

3.1 SEM and EDS Analysis

The SEM characterization presented in Fig. 1 provides insightful observations of natural bentonite (Fig. 1a), PDA-B (Fig. 1b), and PDA-B after uranium adsorption (Fig. 1c). For natural bentonite (Fig. 1a), the surface appears smooth, flat, dense, and free from cracks. In contrast, PDA-B (Fig. 1b) exhibits a surface covered with granular polydopamine protrusions, which are densely arranged, resulting in a rough and textured appearance. This marked contrast in surface structure between natural bentonite and PDA-B underscores the significant changes that occur upon dopamine hydrochloride modification. It suggests that PDA-B offers a greater number

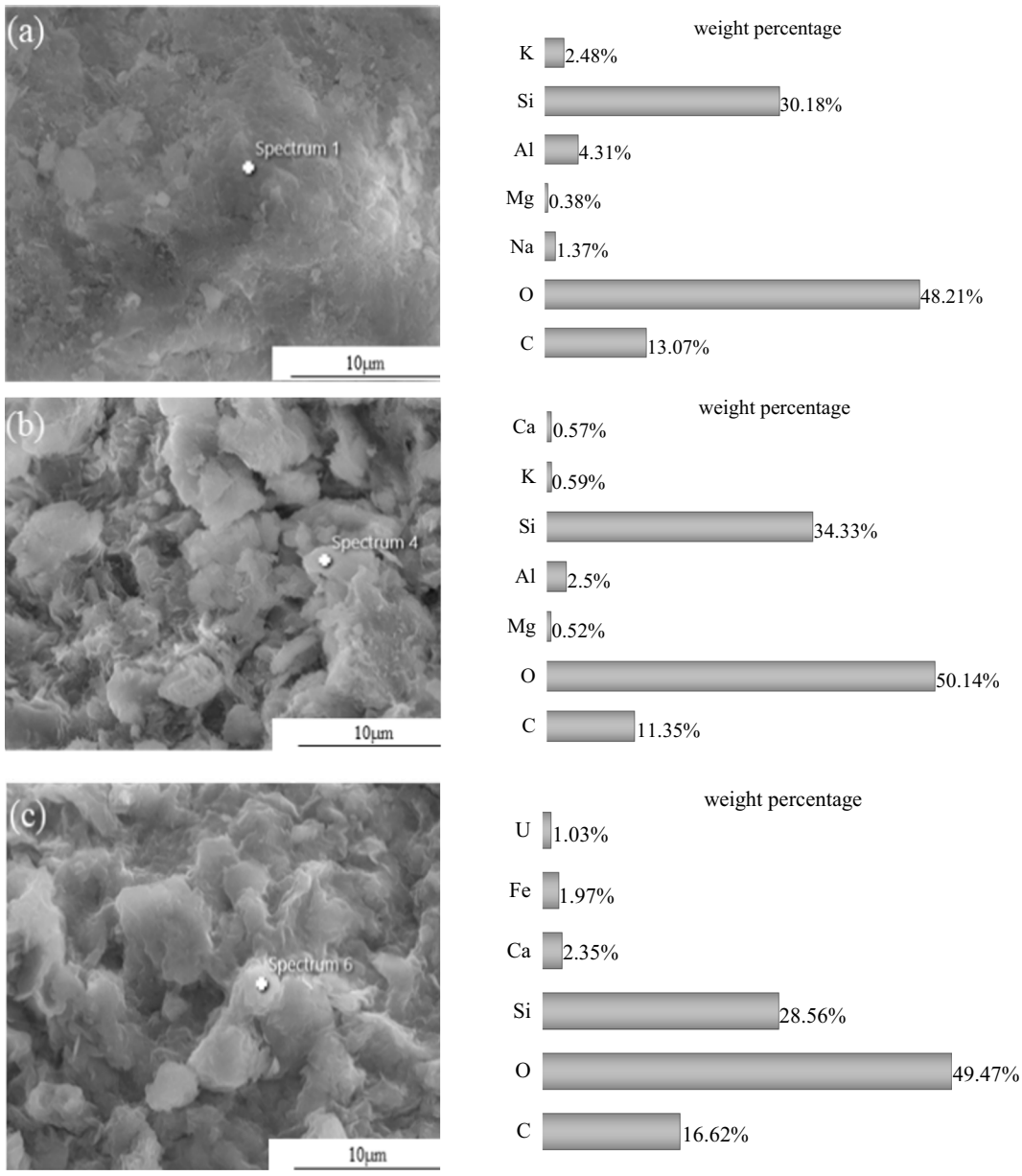

Fig. 1 The SEM and EDS of PDA-B: a is natural bentonite, b is PDA-B, c is PDA-B after adsorption of uranium

of adsorption sites on its surface, thereby enhancing its adsorption capacity, particularly for low-concentration U(VI). Furthermore, these alterations confirm the successful synthesis of PDA-B. Upon uranium adsorption, the SEM image of PDA-B (Fig. 1c) shows that most of the pores and protrusions become filled, resulting in a denser interior structure. The presence of uranium elements is indicated by EDS analysis, supporting the conclusion that uranium was effectively adsorbed by PDA-B. Additionally, the disappearance of Al and Mg, along with a significant reduction in Si content, suggests the involvement of ion exchange in the adsorption process of PDA-B (Liu et al., 2022; Fu et al., 2021).

3.2 XRD Characterization

The XRD spectrum presented in Fig. 2 offers insights into the crystal structure of bentonite before and after modification with dopamine hydrochloride and uranium adsorption. In the XRD patterns, it's evident that the crystal structure of bentonite remained largely unchanged after modification with dopamine hydrochloride and subsequent uranium adsorption. This observation suggests that both modification and uranium adsorption had minimal impact on the crystal structure of bentonite. However, a notable difference can be seen in the 001 peak position. In the XRD pattern of PDA-B, this peak shifts toward a smaller angle compared to natural bentonite. This shift indicates an increase in the interlayer spacing of PDA-B. This change is likely attributed to ion exchange processes involving dopamine hydrochloride and the calcium ions within the interlayer of bentonite (Fu, X., 2021). Upon uranium adsorption by PDA-B, the 001 peak position shifts toward a larger angle when compared to the pre-adsorption state. This shift corresponds to a decrease in the interlayer spacing. This suggests that uranium was effectively adsorbed by PDA-B, although the change in the shift angle is minimal. This observation implies that uranium's entry into the interlayer spacing was relatively limited. The primary adsorption mechanism appears to involve chelation and coordination between uranyl ions and the functional groups present on the material's surface, with physical adsorption playing a minor role (Xia et al., 2013).

3.3 Effect of Ph, Temperature and Initial Concentration

Figure 3(b) demonstrates that PDA-B exhibits a broad pH tolerance range and shows superior removal efficiency within the pH range of 4 to 9. This adaptability surpasses that of the Fe0-PRB material (Zhou et al., 2018) suggests its potential application in real-world scenarios for uranium-containing wastewater treatment, which can contribute to enhancing the environmental quality around tailings ponds. As pH values of the solution increase, the removal efficiency of U(VI) by PDA-B initially rises, stabilizes, and then declines. This pH-dependent trend can be explained by the speciation of uranium in solution and the surface charge characteristics of PDA-B. At strongly acidic pH, U(VI) primarily exists in the form of UO_2^{2+}, while the active sites on PDA-B are protonated, leading to a positively charged surface. Electrostatic repulsion between UO_2^{2+} and the protonated PDA-B surface hinders the adsorption process. Additionally, excessive H^+ ions compete with uranyl ions, further reducing the removal rate (Wang, 2023). With an increase in pH within the appropriate range, PDA-B undergoes deprotonation and becomes negatively charged, promoting the formation of

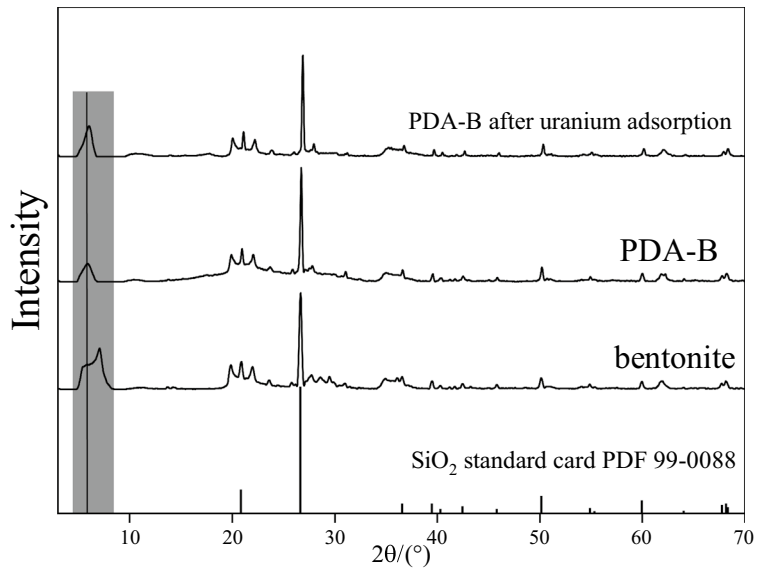

Fig. 2 The XRD of PDA-B before and after adsorption and original bentonite

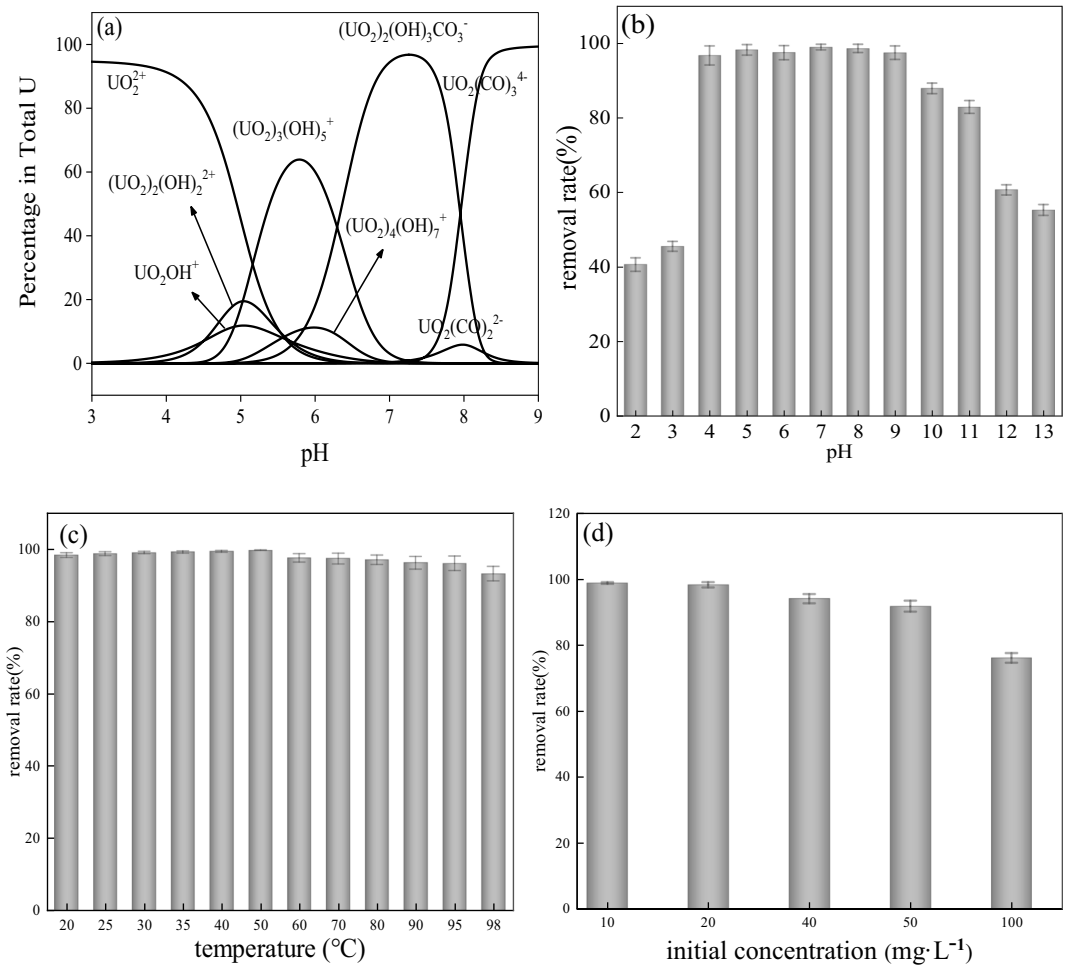

Fig. 3 (a) The existing form of uranium at different pH; (b) Influence of pH; (c) Influence of temperature; (d) Influence of initial concentration

positively charged uranyl complexes like UO_2OH^+, $(UO_2)_2OH_2^{2+}$, and $(UO_2)_3(OH)_5^+$, thereby strengthening the electrostatic attraction between the surface of PDA-B and uranium ions and improving the adsorption efficiency (Chen et al., 2022). However, when the pH becomes too high, most U(VI) exists as $[(UO_2)_8O_2(OH)_{12}\cdot 12H_2O]$ and in the form of $UO_2(CO_3)_2^{2-}$ and $UO_2(CO_3)_4^{3-}$, which are less amenable to adsorption on PDA-B. Excessively high pH can lead to precipitation and reduce the concentration of uranium in the solution to below 10 mg/L, affecting subsequent adsorption processes. In this case, the removal effect is a combination of adsorption and precipitation, which has an adverse impact on subsequent adsorption processes. pH values greater than 8 result in UO_2^{2+} hydrolysis with abundant OH- ions, forming $UO_2(OH)_2$ precipitates, further diminishing adsorption efficiency (Wang et al., 2022). To maintain the removal rate while avoiding the complications introduced by overly high or low pH values, subsequent tests were conducted with a solution at pH 7. This choice aligns with both wastewater discharge standards and the findings of this section. The rule established here closely resembles the pH-dependent uranium adsorption observed in previous studies, such as Zhao et al.'s work on amidoxime magnetic graphene oxide composites (Zhao et al., 2013) and Wang et al.'s study using biochar for uranium-containing wastewater treatment (Wang et al., 2021).

In both of these studies, the pH value significantly influenced the adsorption behavior of U(VI), demonstrating the importance of carefully controlling pH during testing.

As depicted in Fig. 3(c), the comprehensive assessment of U(VI) removal by PDA-B reveals that the removal efficacy remains relatively unaffected by temperature variations, showcasing a robust temperature adaptability. When implemented for the treatment of real uranium-containing wastewater, it achieves superior removal rates without the need for external heating, thereby reducing treatment costs and aligning with China's green environmental protection standards. Initially, the removal efficiency exhibited a gradual increase with rising system temperature, but as the temperature continued to escalate, the removal effect decreased. These observations can be attributed to the likelihood that increased system temperature heightens the surface activation of the PDA-B adsorbent. This leads to an expansion of active adsorption sites on the material's surface and an enhancement in the efficiency of chelation by its surface functional groups, resulting in a slight increase in removal efficiency with rising temperature (Zhang et al., 2015; Fu, 2021). Furthermore, elevated system temperature reduces the water's viscosity coefficient, consequently increasing the diffusion rate of U(VI) within the system. This facilitates enhanced contact between U(VI) and PDA-B, thereby improving the adsorption effect. However, excessively high temperatures may cause the adsorbed U(VI) to detach from the PDA-B's surface due to the heightened migration rate (Lu et al., 2018), resulting in a corresponding reduction in U(VI) removal efficiency. Hence, subsequent tests were conducted at room temperature without the need for system heating. Notably, Li Ziming (Li et al., 2022) employed loofah for U(VI) adsorption and found that a temperature of 60 °C was required for optimal removal efficiency. In this study, a 100% removal efficiency was achieved at room temperature, highlighting the capacity to achieve higher U(VI) removal rates and adsorption capacities without the need for external temperature control.

The aforementioned experiments have explored the removal of low-concentration uranium from the environment using PDA-B, yielding favorable removal rates and adsorption capacities. The initial uranium concentration in discharged nuclear industrial wastewater is typically relatively high, with reductions occurring only after a certain period in the environment. Consequently, it holds great significance to investigate the impact of the initial uranium concentration on PDA-B. As illustrated in Fig. 3(d), an increase in the initial uranium concentration from 10 mg/L to 100 mg/L results in a continuous decrease in the uranium removal rate by PDA-B, accompanied by an increase in adsorption capacity. This observed trend aligns with the adsorption behavior of different U(VI) concentrations studied by Wang on wheat straw (Wang et al., 2012). Domestic literature (Chen et al., 2016) also reported a similar outcome in their investigation of uranium adsorption using hydroxyl iron-intercalated bentonite. This pattern can be attributed to the concentration gradient between U(VI) in the solution and PDA-B, which becomes more pronounced as the initial concentration of U(VI) rises, creating a stronger driving force between the two. This enhanced interaction between uranium and the adsorbent augments adsorption capacity. However, given the fixed dosage, there is a limitation on the adsorption sites available on PDA-B (Wang et al., 2012). Consequently, when the initial U(VI) concentration surpasses a certain threshold, the adsorption sites on PDA-B gradually become saturated, leading to a decline in removal rates as the remaining uranium in the water body is no longer adsorbed.

3.4 Adsorption model

The isothermal adsorption experiments were conducted under the following conditions: a mass ratio of dopamine hydrochloride to bentonite of 1:10, pH maintained at 7, a dosage of 2 g/L, and testing at room temperature. The samples were placed on a shaker, operated at 150 r/min for 300 min. Various initial mass concentrations of uranium were tested for the purpose of fitting isothermal adsorption curves. The results of these experiments are presented in Fig. 4.

The isothermal adsorption curve elucidates the distribution of U(VI) between the liquid phase and PDA-B when U(VI) reaches adsorption equilibrium within PDA-B, providing insights into the adsorbent's capacity. To better characterize PDA-B's adsorption performance for U(VI), Langmuir and Freundlich models were employed to fit the adsorption process. The fitting results of the adsorption isotherm equations are presented in Fig. 4 and Table 1.

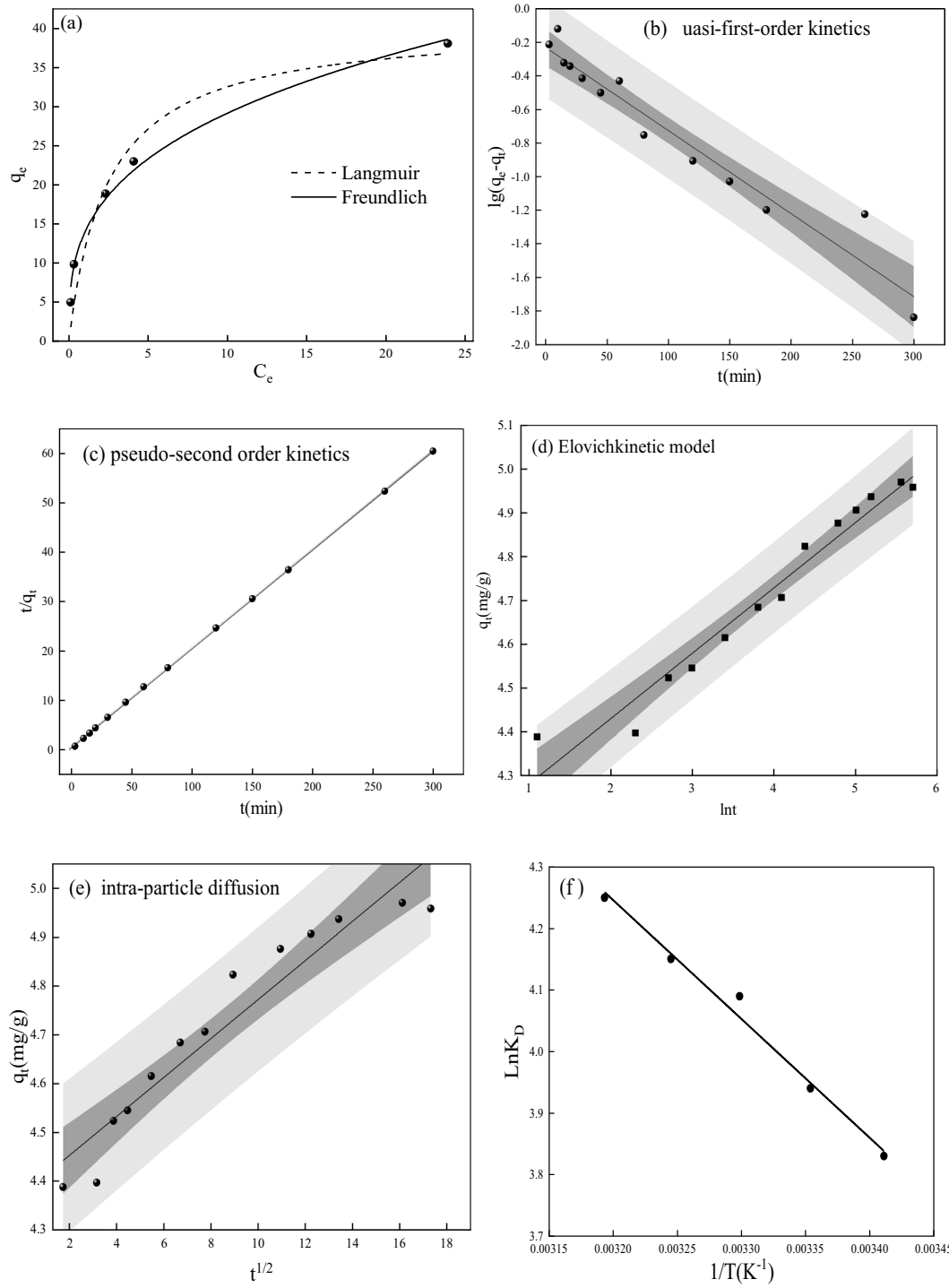

Fig. 4 (a) Isothermal adsorption fitting; (b ~ e) Adsorption kinetics fitting (The dark shadow represents a 95% confidence band, and the light shadow is a 95% prediction band.); (f) Adsorption thermodynamics fitting

Table 1 Fitting parameters of isothermal adsorption model

Temperature (K)	Langmuir isotherm adsorption model			Freundlich isotherm adsorption model		
	Q_m (mg/g)	k_L (L/mg)	R^2	1/n	k_F	R^2
Room temperature	40.59369	0.4035	0.93477	0.32288	13.86775	0.99133

Table 1's R^2 values indicate that the adsorption of U(VI) by PDA-B adheres to both the Langmuir and Freundlich models. However, the Freundlich model fitting is more appropriate, signifying non-uniform surface adsorption of U(VI). The maximum adsorption capacity (Qm) calculated from the fitting is 40.5937 mg/g, which closely aligns with the experimental measurement of 39.0833 mg/g. Moreover, the value of 1/n is less than 1, indicating favorable adsorption conditions.

Under the conditions of a mass ratio of dopamine hydrochloride to bentonite of 1:10, pH at 7, a dosage of 2 g/L, and room temperature, samples were agitated at 150 r/min for various durations with a U(VI) concentration of 10 mg/L for kinetic fitting. The test results are presented in Fig. 4. Figure 4 and Table 2 illustrate that the fitting of the adsorption data is better described by pseudo-second-order kinetics compared to the quasi-first-order kinetics. This suggests that the adsorption process does not solely involve a single-layer adsorption completed by boundary diffusion, supporting the compatibility of the isothermal adsorption model with the Freundlich model's fitting results. In Table 2, it is evident that for uranium adsorption by PDA-B at room temperature, the R^2 value for the pseudo-second-order kinetic fitting is close to 1, signifying a substantial improvement over the pseudo-first-order kinetic and intraparticle diffusion models. According to the pseudo-second-order kinetic equation $t/q_t = 0.20033t + 0.427$, the theoretical equilibrium adsorption capacity for 10 mg/L uranium is 4.99 mg/g, while the experimental uranium adsorption capacity at 300 min is 4.96 mg/g. The relative deviation is merely 0.3015%, indicating that pseudo-second-order kinetics most accurately describe the uranium adsorption process by PDA-B. This suggests that uranium adsorption by PDA-B is chemically controlled, potentially involving electron sharing and electron transfer between PDA-B and uranium. The overall adsorption process may be assumed to be a composite process comprising external liquid film diffusion, surface adsorption, and intraparticle diffusion.

The fitting correlation coefficient for the Elovich model is 0.9572, further validating the results of the pseudo-second-order kinetics and confirming that PDA-B's control of uranium adsorption is through chemical adsorption. The intraparticle diffusion model is used to investigate the rate-controlling step of the adsorption rate. Figure 4 (d) indicates that the fitting curve does not pass through the origin, implying that internal diffusion predominantly controls the overall adsorption process. However, it is not the sole rate-limiting step, and the adsorption rate may also be influenced by liquid film diffusion and surface adsorption (Liu et al., 2000).

Under the given conditions, where the mass ratio of dopamine hydrochloride to bentonite is 1:10, pH is set at 7, and the dosage is 2 g/L, experiments were conducted at various temperatures. The samples were agitated on a shaker at 150 revolutions per minute for 300 min, with the initial U(VI) concentration maintained at 10 mg/L for the purpose of thermodynamic fitting. The graphical representation of the test results can be found in Fig. 4. Following the thermodynamic fitting process, the correlation coefficient was

Table 2 Fitting parameters of adsorption kinetics

Quasi-first-order kinetic model			Pseudo-second order kinetics model			Elovich kinetic model			Intraparticle diffusion model	
k_1 (min^{-1})	q_e (mg/g)	R^2	k_2 [g/(mg·min)]	q_e (mg/g)	R^2	A (mg/g·min)	B (g/mg)	R^2	kp [mg/(g·$min^{1/2}$)]	R^2
0.0049	0.5820	0.9174	0.094	4.99	0.9999	2.35	6.695	0.9572	0.03996	0.9243

determined to be $R^2 = 0.9981$. The calculated values for ΔS, ΔH, and ΔG are presented in Table S3. Notably, ΔG is less than zero, indicating that the adsorption process of PDA-B for low concentration U(VI) is an endothermic reaction. This observation is further supported by the fact that ΔG falls outside the range of -20 to 0 kJ·mol^{-1}, as reported in reference (Sun et al., 2017). These results suggest the formation of a new chemical bond, and the interaction forces involved include not only van der Waals forces but also chemical adsorption. This finding aligns with the results obtained from pseudo-second-order kinetics fitting. Furthermore, the positive value of ΔH (> 0) suggests that the adsorption process of PDA-B for low concentration U(VI) is indeed an endothermic reaction, and the Gibbs free energy increases as the temperature rises, in line with reference (Pino et al., 2018). Additionally, this confirms that bentonite exhibits ion exchange properties, thereby providing a theoretical basis for its chemical modification.

3.5 FTIR Analysis

In Fig. 5, the absorption peaks at 3624 cm^{-1} and 3437 cm^{-1} correspond to the stretching vibration absorption peak of bentonite Al–OH and the bending vibration absorption peak of interlayer water -OH, respectively. There is no significant absorption peak in the 3000–1700 cm^{-1} range. The peaks at 1634 cm^{-1}, 1036 cm^{-1}, 795 cm^{-1}, and 467 cm^{-1} respectively represent the bentonite O–H bending vibration absorption peak, Si–O-Si asymmetric stretching vibration absorption peak, Al-O bending absorption peak, and Si–O stretching and bending vibration (Fu, 2021). Following the modification of bentonite with dopamine hydrochloride, the disappearance of the absorption peak at 1589 cm^{-1} may be due to the introduction of a cyano group. A weak absorption peak at 1521 cm^{-1} appears, likely caused by the N–H stretching vibration in the -NH_2 group or the N–H bending vibration in the amide II band. The characteristic peaks of dopamine hydrochloride at 2927 cm^{-1} and 2854 cm^{-1}, related to C = C stretching vibration (Hong et al., 2014), indicate the successful synthesis of PDA-B. After the adsorption of uranium, the C = C peak is noticeably weakened. The absorption peak at 1521 cm^{-1}, associated with -NH_2, shifts to 1535 cm^{-1}, suggesting the involvement of carbonyl and amino groups in uranium adsorption. The weak peak at 1439 cm^{-1}, representing O–H bending vibration, disappears, indicating that uranium may occupy the O–H sites, leading to a weakening of intramolecular O–H hydrogen bonding. This implies that ion exchange and the formation of stable uranium complexes with surface O–H groups on PDA-B are potential mechanisms (Liu et al., 2022). The above analysis supports the earlier adsorption kinetics fitting results, indicating that the primary adsorption mechanism

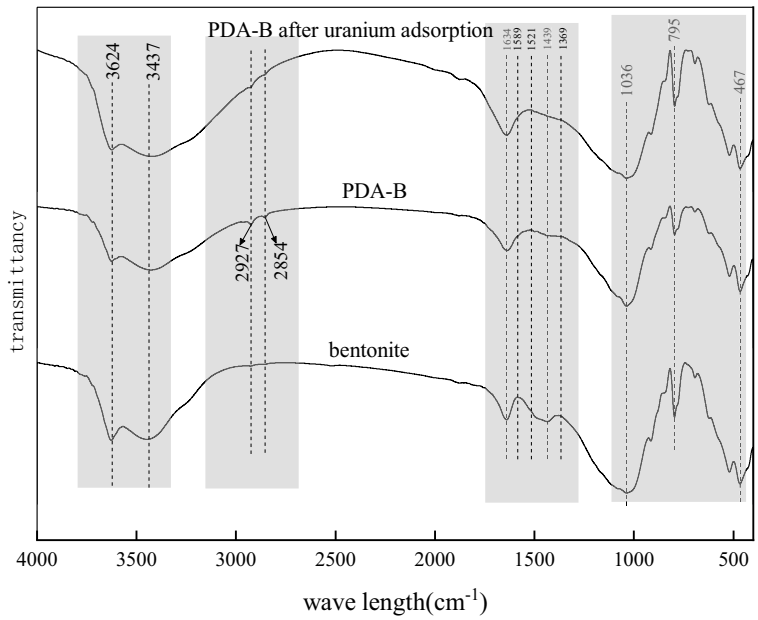

Fig. 5 Infrared spectra of bentonite and PDA-B before and after

of PDA-B is chemical adsorption. This conclusion aligns with the XPS analysis and underscores the significant roles of carbonyl, amino, and hydroxyl groups in uranium adsorption by PDA-B.

adsorption of uranium

3.6 Potential Analysis

The Zeta potential of natural bentonite and PDA-B was analyzed before and after uranium adsorption at pH = 7, and the results are presented in Table 3.

From Table 3, it is evident that both natural bentonite and PDA-B exhibit negative potentials, indicating their capacity to adsorb positively charged U(VI). Notably, the potential value of PDA-B is significantly higher than that of natural bentonite, which can be attributed to the increased presence of surface functional groups. Subsequent to uranium adsorption, both materials undergo changes in potential values, which can be attributed to the adsorption of U(VI). Hence, electrostatic attraction also plays a role in the adsorption process of PDA-B.

Table 3 zeta potential characterization

material	Natural bentonite before adsorption	ntural bentonite after adsorption	PDA-B before adsorption	PDA-B after adsorption
potential	-8.71	-8.14	-12.64	-10.75

3.7 PDA-B Reusability

Material reusability is a crucial factor for cost control, and therefore, investigating the repeatability of PDA-B holds significant research value. Given that acidic conditions were found to be less favorable for PDA-B adsorption, a suitable concentration of hydrochloric acid was employed for desorption regeneration tests. As depicted in Fig. 6, even after four cycles of adsorption and desorption experiments, PDA-B maintained a uranium removal rate of over 80%. On the fifth desorption cycle, the uranium removal rate by PDA-B stood at 74.16%, still demonstrating a notable adsorption capacity. This underscores the exceptional reusability of PDA-B. The observed decrease in removal efficiency can be attributed to the acid desorption process, which causes the detachment of dopamine hydrochloride from PDA-B, thereby affecting its adsorption performance. This observation aligns with the TOC test results, providing further confirmation.

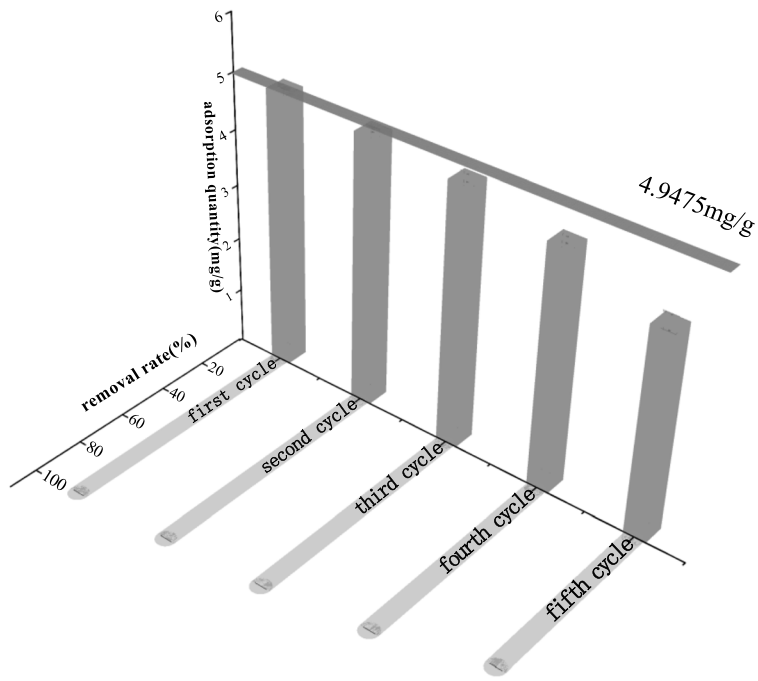

Fig. 6 PDA-B reusability and stability test

3.8 Adsorption Mechanism of PDA-B

The adsorption of U(VI) by PDA-B appears to involve several mechanisms:

(1) Physical Adsorption**:** Bentonite's specific surface area and pore structure provide adsorption sites for U(VI), facilitating ion exchange. This physical adsorption process contributes to U(VI) removal.

(2) Chemical Adsorption**:** Dopamine hydrochloride, due to its numerous functional groups, can modify bentonite to introduce carbonyl, amino, and hydroxyl groups. Uranium, in turn, can provide vacant orbitals for lone pair electrons from these functional groups. This interaction enables PDA-B to coordinate with U(VI) through chemical adsorption, enhancing its adsorption capacity (Shen et al., 2013).

(3) Electrostatic Adsorption**:** As evident from the pH sensitivity of PDA-B, both strong acidic and alkaline conditions impact its adsorption behavior. Better removal efficiency is achieved under weak acidic and weak alkaline conditions. Based on zeta potential characterization, PDA-B carries a negative charge at a neutral pH. This charge interaction allows for electrostatic adsorption between uranyl ions and the negative charges within the PDA-B structure. Figure 7.

4 Conclusion

Bentonite was successfully modified by hydrochloric acid dopamine using a simple one-step hydrothermal method, and the characterization of the modified bentonite was performed. When applied to low-concentration uranium-containing wastewater, PDA-B demonstrated an impressive removal rate exceeding 98% and exhibited excellent recyclability. These outcomes underscore the substantial practical application potential of PDA-B. Mechanism analysis suggests that the adsorption of uranium by PDA-B encompasses physical, chemical, and electrostatic interactions. However, the primary adsorption mechanism involves the chelation and coordination of functional groups, notably carbonyl, amino, and hydroxyl groups. Furthermore, it's worth highlighting that the preparation process for PDA-B is straightforward, cost-effective, and conducive to potential reuse. As a result, PDA-B holds significant promise as an environmentally friendly and cost-effective material for the adsorption and removal of low-concentration uranium-containing wastewater.

In the future, there is potential for further research and development of more efficient adsorbents based on dopamine-modified bentonite. By controlling the structure of bentonite and the modification method of dopamine, the adsorption capacity and rate for uranium can be enhanced, thus achieving more effective management of uranium contamination. Alternatively, optimization of the process for uranium adsorption using dopamine-modified bentonite can be pursued to reduce energy consumption and the use of chemical reagents, thereby enhancing the environmental friendliness and sustainability of the technology. Furthermore, exploration of the integration of

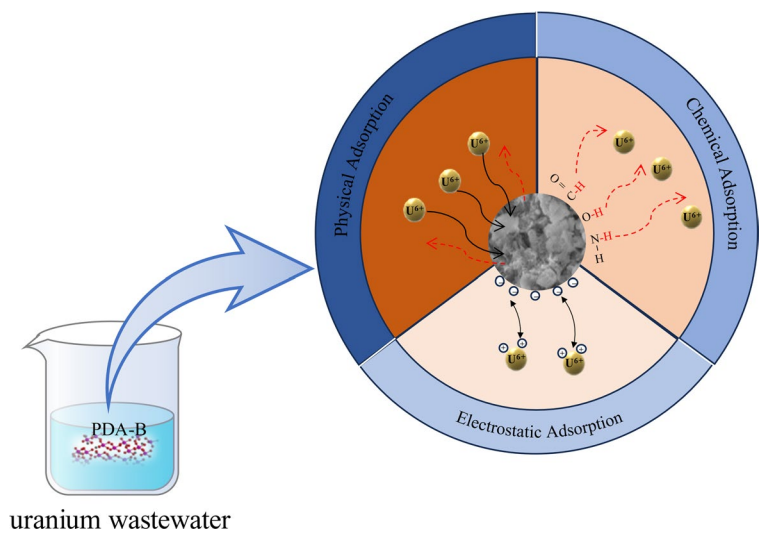

Fig. 7 Possible mechanisms for uranium (VI) removal by PDA-B

this technique with other green environmental technologies, such as phytoremediation and biodegradation, can diversify and comprehensively address uranium pollution.

Author Contribution Longxiang Li: methodology, investigation, writing—original draft. Zhongkui Zhou: funding acquisition, supervision, writing—review and editing. Yadan Guo and Yishuo Zhang: writing—review and editing. Yi Zhao and Yan Xin: investigation.

Funding This work was supported by The National Natural Science Foundation of China funded project, (41662024) and Key project of key research and development plan in Jiangxi Province (20212BBG71011).

Data Availability The datasets used and/or analyzed during the current study are available from the corresponding author on reasonable request.

Declarations

Ethics Approval Not applicable.

Consent to Participate All the authors listed have approved the manuscript.

Consent for Publication This manuscript is approved by all authors for publication in Water, Air, & Soil Pollution.

Competing of Interests The authors declare no competing interests.

References

Chen, J., Xie, S., Zeng, T., Ling, H., & Wang, L. (2016). Preparation of hydroxyl iron intercalated bentonite and its adsorption characteristics and mechanism for uranium (VI). *Acta Materiae Co mpositae Sinica, 33*(11), 2649–2656. https://doi.org/10.13801/j.cnki.fhclxb.20160229.004

Chen, Y., Zhou, T., Zhang, H., Tan, J., Li, K., Wu, T., & Deng, Q. (2023). Decomposition of Litterfall and Evaluation of Uranium Release and Secondary Contamination from Uranium Tailings Ponds. *Water, Air, and Soil Pollution, 234*, 636. https://doi.org/10.1007/s11270-023-06654-5

Chen, Y., Quan, Z., Wang, W., Liu, X., Wang, Y., Chen, L. (2022). Preparation of Zn / Mn / PAA and adsorption of uranyl ion. *Fine chemicals,* 39(05):1004–1011+1019. https://doi.org/10.13550/j.jxhg.20211250

Fu, X. (2021). Study on the adsorption of heavy metal ions in water by carboxylated bentonite. *Harbin Instituteof technology, 2021*, 32–38. https://doi.org/10.27061/d.cnki.ghgdu.2021.004756

Hong, S., Schaber, C. F., & Dening, K. (2014). Catecholamine: Air/Water Interfacial Formation of Freestanding, Stimuli-Responsive, Self-Healing Catecholamine Janus-Faced Microfilms (Adv Mater 45/2014). *Advanced Materials, 26*(45), 7534–7534. https://doi.org/10.1002/adma.201403259

Li, Z., Chen, S., Su, Y., Gou, Y., Song, Y., Chang, H., Wang, F., & Wu, H. (2022). Experimental study on modification of luffa sponge and its adsorption of uranium from seawater. *Hydrometallurgy of China, 41*(03), 213–220. https://doi.org/10.13355/j.cnki.sfyj.2022.03.007

Lian, L., Guo, L., & Wang, A. (2009). Use of $CaCl_2$ modified bentonite for removal of Congo red dye from aqueous solutions. *Desalination, 249*(2), 797–801. https://doi.org/10.1016/j.desal.2009.02.064

Liu, W., Vidic, R. D., & Brown, T. D. (2000). Impact of flue gas conditions on mercury uptake by sulfur-impregnated activated carbon. *Environmental Science & Technology, 34*(1), 154–159. https://doi.org/10.1021/es990315i

Liu, X., Wang, G., Lei, Y., Xu, M., & Zhang, Y. (2022). Adsorption characteristics of Cu (II) in water by thiol modified corn stover. *China Environmental Science, 42*(03), 1220–1229. https://doi.org/10.19674/j.cnki.issn1000-6923.2022.0062

Lu, Z., Huang, Z., Li, A., Wang, C., Xu, K., He, B., Adilai, A., & Li, J. (2018). Adsorption characteristics of humic acid on heavy metals lead and cadmium. *Acta Scientiae Circ Umstantiac, 38*(09), 3721–3729.

Ma, L., Huang, Y., Deng, H., Yin, H., Tian, Q., Yan, M. (2022). Removal of uranium (VI) from acidic aqueous solutions by fluorapatite. *Journal of Inorganic Materials, 37* (04): 395–405. https://link.cnki.net/urlid/31.1363.tq.20220517.1114.002

Mahadevan, H., Anoop Krishnan, K., Pillai, R. R., & Sudhakaran, S. (2020). Stirring-ageing technique to develop zirconium-pillared bentonite clay along with its surface profiling using various spectroscopic techniques. *Research on Chemical Intermediates, 46*(1), 639–660. https://doi.org/10.1007/s11164-019-03982-2

Pentyala, V. B., & Eapen, S. (2020). High efficiency phytoextraction of uranium using Vetiveria zizanioides L. *Nash. International Journal of Phytoremediation, 22*(11), 1137–1146. https://doi.org/10.1080/15226514.2020.1741506

Pino, L., Vargas, C., Schwarz, A., & Borquez, R. (2018). Influence of operating conditions on the removal of metals and sulfate from copper acid mine drainage by nanofiltration. *Chemical Engineering Journal, 345*, 114–125. https://doi.org/10.1016/j.cej.2018.03.070

Shen, Y., Hu, T., Zeng, G., Huang, D., Yin, L., Liu, Y., Wu, J., & Liu, H. (2013). Degradation of lignocellulose by Penicillium simplicissimum and characteristics of related enzyme activities. *Environmental Science, 34*(02), 781–788. https://doi.org/10.13227/j.hjkx.2013.02.006

Shu, S., Chen, W., Jia, X., & Wang, L. (2021). Adsorption of phenol on CTAB modified iron pillared bentonite. *Bulletin of the Chinese Ceramic Society, 40*(09), 3046–3052. https://doi.org/10.16552/j.cnki.issn1001-1625.20210701.001

Sun, Z., Yan, B., Wang, A., Bai, N., & Li, Y. (2017). Adsorption of Reactive Red X-3B by Chitosan / CTAB Composite Modified Bentonite. *Acta Scientiae Circumstantiae, 37*(02), 617–623. https://doi.org/10.13671/j.hjkxxb.2016.0285

Verma, M., & Loganathan, V. A. (2024). Insights on the Mechanism of Uranium Removal via Nanofiltration in Alkalinity and Salinity Dominated Groundwater Systems. *Water,*

Air, and Soil Pollution, 235, 256. https://doi.org/10.1007/s11270-024-07065-w

Volzone, C., & Garrido, L. B. (2008). Use of modified hydroxy-aluminum bentonites for chromium (III) removal from solutions. *Journal of Environmental Management, 88*(4), 1640–1648. https://doi.org/10.1016/j.jenvman.2007.08.003

Wang, L. (2023). Study on the adsorption performance of U (VI) in wastewater by pomelo peel biochar loaded Mg / Al-LDH. *University of South China*, *43*(01), 163–168. https://doi.org/10.27234/d.cnki.gnhuu.2022.000254

Wang, X., Xia, L., Tan, K., & Zheng, W. (2012). Studies on adsorption of uranium (VI) from aqueous solution by wheat straw. *Environmental Progress & Sustainable Energy, 31*(4), 566–576. https://doi.org/10.1002/ep.10582

Wang, Y., Niu, J., Xu, L., Li, C., Xing, H., Liu, X., & Xu, W. (2021). Preparation of iron-loaded biochar and its application in uranium-bearing mine water treatment. *Hydrometallurgy of China, 40*(04), 310–314. https://doi.org/10.13355/j.cnki.sfyj.2021.04.009

Wang, P., Tan, K., Li, Y., Xiao, W., Liu, Z., Tan, W., & Xu, Y. (2022). The adsorption of U(VI) by albite during acid in-situ leaching mining of uranium. *Journal of Radioanalytical and Nuclear Chemistry, 331*(5), 2185–2193. https://doi.org/10.1007/s10967-022-08254-9

Xia, L., Tan, K., Zheng, W., & Wang, X. (2013). Uranium removal from aqueous solution by banyan leaves: equilibrium, thermodynamic, kinetic, and mechanism studies. *Journal of Environmental Engineering, 139*(6), 887–895. https://doi.org/10.1061/(ASCE)EE.1943-7870.0000695

Xiong, X., Lin, Z., Wang, W., Chen, Q., Zhou, J., Luo, T., & Zhu, Y. (2018). Study on the adsorption of U (VI) in water by iron titanium pillared bentonite. *Uranium Mining and Metallurgy, 37*(04), 296–303. https://doi.org/10.13426/j.cnki.yky.2018.04.013

Zhang, H., Jiang, J., Liu, Y., Xiang, J., & Liu, X. (2015). Adsorption of copper ions in water by rape straw pith and its mechanism. *Chinese Journal of Environmental Engineering, 9*(12), 5865–5873.

Zhang, Y., Zhou, Z., Wang, S., Wang, S., Sun, Z., Hu, Z., Yuan, J., & Fan, X. (2022a). Experiment on removal of U (VI) from water by STAC modified organic bentonite. *Nonferrous Metals (extractive Metallurgy), 01*, 127–132.

Zhang, Y., Zhou, Z., Yang, S., & Li, J. (2022b). Adsorption of U (VI) from low concentration wastewater by CTAB modified bentonite was studied. *Hydrometallurgy of China, 41*(02), 145–149.

Zhao, Y., Li, J., Zhang, S., Chen, H., & Shao, D. (2013). Efficient enrichment of uranium (VI) on amidoximated magnetite/graphene oxide composites. *RSC Advances, 3*(41), 18952–18959. https://doi.org/10.1039/C3RA42236D

Zhou, S., Zhang, J., Liu, Y., Fang. F., Hou, k., Wang, H. (2018). Application and prospect of Fe^0-PRB technology in remediation of uranium contaminated groundwater. *Journal of University of South China (Science and Technology),* 32 (06): 1–8+36.

Zhou, Z., & Xu, S. (2012). Experimental study on the treatment of Cr^{6+} in electroplating wastewater by aluminum pillared modified bentonite Industrial water trea. *Industrial Water Treatment, 32*(12), 55–57.